Development of a Knowledge-Based Optimization Method for Aerodynamic Design

Richard L. Campbell and Michelle N. Lynde
NASA Langley Research Center, Hampton, Virginia, US

Abstract

A new aerodynamic design method, CODISC, has been developed that combines an existing knowledge-based design method, CDISC, with a simple optimization module known as SOUP. The primary goal of this new design system is to improve the performance gains obtained using CDISC without adding significant computational time. An additional benefit of this approach is a reduction in the need for *a priori* knowledge of good initial input variable values as well as for subsequent manual revisions of those values as the design progresses. A series of 2D and 3D test cases are used to illustrate the development of the process and some of the options available at transonic and supersonic speeds for both laminar and turbulent flow. The test cases start from good baseline configurations and, in all cases, were able to improve the performance. Several new guidelines for good initial values for the design variables, as well new design rules within CDISC itself, were developed from these cases.

Nomenclature

AOWDG	=	Aerodynamic Optimization Workshop Discussion Group
c	=	Chord length
CART3D	=	Cartesian 3D, Euler flow solver
CDISC	=	Constrained Direct Iterative Surface Curvature, design module
CF	=	Crossflow
CFD	=	Computational Fluid Dynamics
C_D	=	Configuration drag coefficient
c_d	=	Sectional drag coefficient
C_L	=	Configuration lift coefficient
c_l	=	Sectional lift coefficient
CMOPT	=	CDISC flow constraint, optimizes sectional pitching moment
CODISC	=	Constrained Optimization Direct Iterative Surface Curvature, design system
C_P	=	Pressure coefficient
CRM	=	Common Research Model
D0	=	Supercritical airfoil test case
LASTRAC	=	Langley Stability and Transition Analysis Code, transition prediction software
LP	=	MUD constraint chordwise loading input variable
MUD	=	CDISC flow constraint, Modified Uniform Distribution of lift
NJWB	=	NASA/JAXA Wing Body, supersonic configuration test case
NLF	=	Natural laminar flow
SOUP	=	Simple Optimization Utility Program, optimization module
SSNLF	=	CDISC flow constraint, Supersonic Natural Laminar Flow
TetrUSS	=	Tetrahedral Unstructured Software System, flow solver package
TS	=	Tollmien-Schlichting
UDF	=	Universal damping function, CDISC NLF design parameter
USM3D	=	Unstructured Mesh 3D, Navier-Stokes flow solver
x/c	=	x-location nondimensionalized by local chord
X_{ca}	=	x/c location of end of crossflow attenuation region in SSNLF target pressure
X_{tr}	=	x/c location of transition in SSNLF target pressure
X_{shk}	=	x/c location of shock in SSNLF target pressure
η	=	Semispan location

Introduction

The use of automated CFD-based aerodynamic design methods has become the norm in the aircraft design process. With the improvements in aerodynamic analysis and design software, as well as computer systems architecture and hardware, the time required for a design has come down to a point that these methods are being used earlier in the design process, including in the conceptual design stage. While the majority of the new methods are based on numerical optimization, the knowledge-based CDISC design method [1] is still fairly widely used in US industry and government research organizations. The primary advantage of CDISC relative to a numerical optimization method is that, because it uses prescribed rather than computed sensitivity derivatives, it typically produces designs in about the same time as the original converged baseline analysis. Even with the use of an adjoint solver to compute these derivatives, optimization often requires 1-2 orders of magnitude more time than CDISC to produce a design. Nongradient-based optimization approaches, such as genetic methods, often require another order of magnitude or more time beyond the gradient-based methods.

A potential drawback of the knowledge-based approach to design is that it requires an *a priori* knowledge, not just of the flow physics that will lead to an improved design, but also of how to adjust the target pressures used in design to obtain the desired improvement. In cases involving transonic transports, this knowledge base has been developed over the last few decades. As an illustration of this, CDISC was used to repeat the design cases for the Aerodynamic Optimization Workshop Discussion Group (AOWDG) W1 wing configuration reported by Vassberg [2]. The CDISC design philosophy was to make the spanload elliptical to minimize induced drag and to reduce shock strengths to decrease wave drag, while meeting other flow and geometry constraints. The final aggregate drag reductions for the multipoint design case from CDISC and the three optimization methods used in [2] are shown in figure 1. As can be seen, CDISC produced comparable drag reductions, but in much less time, as much as a factor of 500 in one case.

The CDISC method uses flow constraints to generate target pressures based on design rules that have been developed from applications for a variety of configurations. Typically, the initial values of the input parameters are chosen based on previous experience, then are manually adjusted after several design cycles based on how the geometry, as well as the flow characteristics, are developing. While this manual adjustment procedure has provided good results for a number of designs in the past, it is proposed that a more effective and efficient approach would be to use optimization to determine the best CDISC input parameters.

This simple optimization approach with CDISC was first demonstrated by Campbell [3] for a transonic airfoil design. A more rigorous, proprietary method, known as KNOPTER, was developed by researchers at Lockheed Martin and was successfully applied to several of their configurations [4,5]. For our new implementation of this approach, an auxiliary code, SOUP (Simple Optimization Utility Program), has been created that adjusts the input parameters for selected CDISC flow constraints to try to reduce the drag of the configuration.

This hybrid approach, referred to as CODISC, is consistent with the overall emphasis on efficiency in CDISC, with three main objectives in its implementation. The primary objective is to improve the effectiveness of CDISC in terms of drag reduction. Even though CDISC often provides results that are comparable to those from numerical optimization, the target pressure architectures created by the flow constraints are not necessarily optimal. It is hoped that automatically adjusting one or more of the input parameters will provide some additional drag reduction and perhaps lead to new design rules that could reduce the need for these adjustments for future designs. The second objective is to retain as much of the original CDISC efficiency as possible, hopefully achieving optimized designs in less than 5x the time needed for the baseline analysis, or approximately double the time for a standard CDISC design. The final goal is to reduce the knowledge base required of the user in setting up the input for a design. While some

input parameters have recommended values, these are increasingly less likely to be optimum for configurations that do not resemble the standard tube-and-wing transport aircraft used to develop the suggested values. With the new approach, it should be less important that the configuration coming out of conceptual design have refined wing twist and airfoil shapes.

This paper will focus on the development of the process and design rules for the new CODISC design system, while a companion paper, "Application of a Knowledge-Based Optimization Method for Aerodynamic Design" by Lynde and Campbell, will assess the system in the more typical 3-D viscous design environment. The test cases chosen generally start from a refined baseline to provide a more rigorous test of the method.

Methods

Flow solvers

A flow chart of the CODISC design system is shown in figure 2. The modular coupling of the original CDISC system has been retained to allow the use of multiple flow solvers and gridding approaches. For the examples included in this paper, two flow solvers were used. The first one is the CART3D Euler code [6] that utilizes Cartesian grids to provide both ease of setup and efficiency. It was selected to provide a rapid assessment of CODISC for supersonic design, where viscous effects do not have a strong influence on the design pressures. The second flow solver used is the USM3D code from the TetrUSS software system [7] that solves the Navier-Stokes equations on tetrahedral unstructured grids. One-cell wide quasi-2D grids were used for transonic airfoil design cases to provide a quick means of developing the optimization process and evaluating various design options before moving to a full 3D viscous design. The Spalart-Allmaras turbulence model [8] was used for all cases in this paper and the forced-laminarization option [9] was invoked to place boundary layer transition at the location specified by the CODISC process for NLF design cases.

SOUP

The Flow/Geometry Extraction module has been modified to provide the global force and moment information required by the SOUP module, as well as the surface geometry, pressures, and skin-friction data at the design stations utilized by CDISC. This information is passed to the SOUP code, along with the CDISC target file, where it is used to drive the adjustment of selected input parameters for some of the CDISC flow constraints. In addition to the global force and moment information, local values of lift and drag at each design station are also computed from the surface geometry, pressure, and skin-friction information. These local forces allow for the independent adjustment of the optimization parameters at each design station.

The SOUP module is called before CDISC in each CODISC design cycle; however, the optimization variable is only updated if the current lift coefficient is within a user-specified variation (convergence band) around the design lift coefficient. An option is available in SOUP to adjust the desired section lift coefficients in the target file to move the total lift toward the design value without altering the configuration angle of attack. This option was used in all of the cases presented in this paper. An alternate approach would be to use lift matching in the flow solver itself.

Another option included in SOUP is the adjustment of the drag value used to drive changes to the optimization variable to try to account for any transitory mismatch to the design lift. This approach allows changes to be made early in the optimization process without requiring the full convergence of either the flow solution or the CDISC design, similar to the traditional CDISC parallel convergence approach. The CODISC process continues until one of the following conditions are met: 1) a normal minimum is found,

where the corrected drag has increased above the previous minimum value by a specified amount; or 2) a flat minimum is detected, where the corrected drag has remained within a specified variation for at least 10 optimization cycles. For both of these stopping criteria, the lift also must have remained within its specified tolerance for at least 10 cycles. The specified values for the normal and flat minimums should be large enough to avoid early termination due to any noise in the drag versus design cycle data.

CDISC

Currently, three CDISC flow constraints can be adjusted by SOUP. The first one is the Modified Uniform Distribution (MUD) constraint that adjusts the chordwise loading forward or aft at a design station based on the input loading parameter LP (see figure 3). At LP = 0, the chordwise loading is fairly uniform, with blending to the current analysis pressures occurring near the leading and trailing edges, controlled by two other input parameters. This constraint has mainly been used for subsonic and supersonic cases where strong pressure discontinuities, such as shocks, are not present.

The second flow constraint used in optimization is the Supersonic Natural Laminar Flow (SSNLF) constraint. Though originally developed for natural laminar flow (NLF) design for supersonic configurations [10], it has been modified for use at transonic conditions [11-13] for both laminar and turbulent design cases. The SSNLF parameterization for a typical transonic NLF case is shown in figure 4. In this figure, X_{ca} marks the end of the rapid acceleration used for crossflow (CF) attenuation and the beginning of the universal damping function (UDF) region, used to control Tollmein-Schlichting (TS) mode growth. The X_{tr} variable is the desired transition location. A mild adverse gradient is prescribed aft of X_{tr} to reduce the shock strength at the termination of the pressure rooftop, X_{shk}.

For NLF optimization, X_{ca} and X_{shk} are set based on empirical design rules, while X_{tr} is adjusted based on the change in drag from the previous design cycle. As the transition location is adjusted, the UDF parameter needs to be modified as well to ensure that the TS growth envelope meets the critical N-factor limit at X_{tr}. Ideally, the required UDF value would be iteratively determined using a boundary layer stability analysis code, but the time needed to do this would be prohibitive. Instead, an empirically-derived relationship that sets the value of UDF based on the chord Reynolds number, desired transition location, and TS critical N-factor has been built into the SSNLF constraint in CDISC to automatically determine UDF.

An assessment of the accuracy of this UDF prediction algorithm is shown in figure 5. The actual X_{tr} values were computed using the LASTRAC boundary layer stability analysis code [14] and the target pressures generated from the SSNLF constraint for values of chord Reynolds number of 20, 30, and 40 million, transition x/c locations from 0.3 to 0.6, and a fixed TS critical N-factor of 10. In the primary region of interest, x/c = 0.4 - 0.6, the predicted and actual values of X_{tr} are fairly close, usually within 0.05c. During design, the transition location is restricted to be at least 0.1c ahead of the shock location to avoid the risk of laminar separation at the shock.

For turbulent flow cases, X_{tr} is moved to be coincident with X_{shk}, with that location based on a blending of the current analysis shock location and a prescribed position based on a function of Mach number. This method has added stability to the design process and is a significant improvement over previous CDISC approaches. This design rule was developed initially using 2D airfoil optimization cases, then modified to account for the sweep and taper present in a 3D wing. It may require further modification for root and tip effects, but these are not included in the present design rule. The UDF variable is optimized during the turbulent flow design, with the resulting pressure rooftop having a slightly concave adverse gradient terminating in a weak shock (see figure 6). Several unpublished applications of the SSNLF constraint for turbulent design, without the SOUP optimization, produced significant drag reductions at the design point with good off-design performance; however, those designs were started from baselines with rather poor

performance. The 2D viscous cases in this paper will start from a more reasonable baseline airfoil and will examine if the SOUP process retains the good off-design performance or produces more of a point design.

A third constraint, CMOPT, has recently been added to CDISC and SOUP to allow optimization of wing section pitching moment for minimum drag. Initial results for this constraint (not included in this paper), indicate that a design rule based on the skin-friction coefficient near the trailing edge of the upper surface may be a viable alternative to direct optimization of the pitching moment. As a note, the pitching moment for the MUD constraint varies linearly with the loading parameter, LP. The SSNLF constraint has an option to adjust the pitching moment based on a design rule to provide a reasonable, but not necessarily optimum, value at each design station based on the local lift coefficient for both 2D and 3D cases.

Examples to illustrate the MUD, as well as both turbulent and laminar SSNLF, design options are included in the next section. When possible, the results will be compared with similar ones obtained using other optimization methods.

Results

Supersonic wing design using the MUD constraint

The first set of design cases use the CART3D Euler flow solver in the CODISC process to try to improve the performance of a generic supersonic transport configuration [10]. This configuration was designed by an expert user (Dr. Matthias Wintzer) using the adjoint optimization capability in CART3D. It served as a baseline in a cooperative NLF design effort between NASA and the Japanese aerospace agency, JAXA, and is referred to as the NASA-JAXA Wing Body (NJWB). A planform view of this configuration is shown in figure 7, with the design stations marked as black or yellow lines. The design conditions for this case are Mach = 1.6 and a lift coefficient of 0.10. The CDISC design retains the spanwise lift, maximum thickness, and leading-edge radius distributions of the baseline, while using the MUD constraint to create the target pressures from the current analysis pressures. This case should provide a significant challenge to the CODISC method as it is already highly refined and there is no guarantee that the basic MUD pressure architecture can be made optimal even with the SOUP adjustments.

To investigate this latter concern, a script was developed to cycle between the SOUP and CDISC modules with no flow solver updates, adjusting the LP variable to minimize the differences between the target and baseline analysis pressures. Examples of the resulting match to the baseline pressure coefficients at stations 3 and 8 are shown in figure 8. The "best fit" LP values across the semispan are shown in figure 9, with the solid blue line displaying a linear fit to the data points. The linearity of the LP values with semispan location (η) suggests that a possible optimization strategy that used global drag would be to drive a linear variation of LP, anchored with LP = 0 at the tip.

A basic CDISC design using the best-fit targets was run and the results are shown in figures 10 -12. Figure 10 shows that the final design retained the original best-fit loading parameter values across the span. In figures 11 and 12, the MUD loading parameter (LP) is the value at station 3, the most inboard station for design. As this is a CDISC-only design, the LP value at every station remains fixed at the best-fit values throughout the design. Because target pressures are very close to the baseline analysis, the lift coefficient remains within the convergence band throughout the design, as seen in figure 11. The C_L convergence band for all of the NJWB design cases is ± 0.0005 from the design value of 0.099. The drag convergence history is shown in figure 12, with the raw values represented by the long red dashes and the drag corrected for lift variation from the design C_L shown as the finely dashed red line. The corrected drag curve flattens near cycle 15 at essentially the same value as the baseline drag, with the raw drag approaching this value later. This convergence is faster than a typical CDISC design (30 cycles for turbulent flow, 50 cycles for an NLF

design), probably because the final targets were very close to the starting conditions. Note that the design cycle axis length (150) represents the desired limit of 5x the length of a typical converged baseline analysis.

Several observations can be made from the results of this case. First, the drag correction approach seems to be reasonable, as the corrected drag stayed fairly constant as the lift converged toward the middle of the band and the raw drag approached the corrected value. A second conclusion is that the MUD pressure architecture is representative of good supersonic wing pressures. While the inboard target pressures were very close to the baseline analysis (figure 8a), the outboard ones (figure 8b) did have some significant differences. It is encouraging that these differences did not have an adverse effect on performance and that a basic CDISC design could match the drag level of a previously optimized configuration.

In the next case, the SOUP optimization module was activated to see if the drag could be reduced below the baseline value. In order to use total drag as the objective function, while also trying to retain the efficiency of the normal CDISC process, it was proposed that the spanwise LP distribution be adjusted by a single design variable. This was implemented as a scaling factor applied to a triangular spanwise LP increment, with the maximum change at the wing root and no change at the tip. The initial spanwise LP distribution was also triangular, similar to the best-fit targets, as shown by the blue circles in figure 13. The slope of the initial triangular distribution was intentionally set to a flatter value than the best-fit case to allow confirmation that the method is working in case the best-fit distribution was also the optimum.

The lift convergence history for this SOUP optimization run is shown in figure 14, with the LP curve again representing the value at station 3, which would be the largest value on the wing because of the triangular distribution. For this case, the lift (green dashed line) went outside the convergence band for about 15 cycles (see figure 14), causing SOUP to skip the update to the design variable in this region. In figure 15, a normal minimum for the corrected drag is seen to occur at cycle 54, with a drag value about 0.00002 (0.2 counts) below the baseline. The red circles in figure 13 show the LP distribution from this cycle. The slope of the line through the circles is similar to the one through the best-fit targets (figure 9), but is translated up, corresponding to slightly forward loading on the wing. While the drag reduction relative to the baseline is fairly small, it does indicate that the SOUP method is able to improve an already refined design and that the simple triangular distribution of LP might be a good starting point for other configurations. This result was obtained in less than 2x the number of design cycles as a normal CDISC-only design.

As a test of the robustness of the CODISC approach, the previous case was repeated, but started from the baseline configuration with all of the wing twist and camber removed. This configuration is referred to as the NCT (no camber or twist) baseline. The spanwise distribution of LP from the design cycle where the minimum drag occurred is shown in figure 16 and is nearly identical to the previous case that started from the original baseline (figure 13). The lift and drag convergence histories are given in figures 17 and 18. As the new baseline was run at the same angle of attack, the initial C_L (0.125) was considerably higher than the design value of 0.099. Figure 17 shows that it required more than 50 cycles to bring the lift within the convergence band to allow the optimization to start adjusting LP. Figure 18 indicates that a drag minimum was detected at cycle 93 with a drag reduction of 0.6 counts, slightly more than obtained when starting from the normal baseline. While it is preferred to have a method that is fully independent of the starting point, the differences in the final results from the two baseline configurations are small, indicating that the CODISC approach is indeed robust.

The two optimization cases described above utilized a single-parameter function driven by total drag to prescribe the spanwise distribution of LP. A final supersonic test case was attempted to evaluate the option in SOUP to use local drag to drive the optimization. As mentioned in the Methods section, this approach integrates the pressure and skin-friction drag at each design station, then adjusts the design variable at each station based on the change in local drag from the previous design cycle. While this method allows for independent adjustment of LP at each station and should drive the sectional drag to minimum values, it

does not account for situations where a change at one station may lead to a slight drag increase at its own location, but would produce a larger drag decrease at a nearby section (favorable interference). Thus, this approach may not produce a minimum in the total drag.

Several attempts were made to run this case, but SOUP was unable to produce stable local drag minima for this test case. Possible reasons for this have been identified and are under investigation. One is that the baseline NJWB configuration is already within a fairly flat minimum drag bucket and the noise in the drag signal is of the same magnitude as optimization changes. Two options for addressing this are additional refinement of the grid and smoothing of the drag values used for derivatives. A second possible reason for the inconsistent results is that the stations are not fully independent and a change at one station may negate an improvement at an adjacent one. Smoothing and/or limiting the variation in the design variable across the span may help to suppress this effect, known as odd-even coupling, by damping transient effects, especially in the early design cycles. A third possible adverse influence is that the lift is being adjusted to try to match the design value and, even though an adjustment is made to the local values of drag to try to compensate for the current lift offset, the correction is only an approximation and any oscillations in lift will still affect the drag values.

Supercritical airfoil design

Historically, the primary application of CDISC has been in the area of transonic design. As a means of providing rapid turnaround in the development of SOUP, as well as any extensions to CDISC for this type of design, it was decided to perform the initial evaluations using a generic supercritical airfoil and quasi-2D grids with the USM3D flow solver. An assessment of the final CODISC system for 3D viscous wing optimization for both turbulent and laminar flow cases is documented in a companion paper, "Application of a Knowledge-Based Optimization Method for Aerodynamic Design" by M. Lynde and R. Campbell. This paper includes an additional evaluation of the local drag option in an application to laminar flow design for a transonic transport.

The baseline for the following cases is the D0 airfoil [15], run at a Mach number of 0.76, a lift coefficient of 0.7, and a chord Reynolds number of 40 million. This Reynolds number is slightly higher than the one used in [15] (30 million) and was chosen as more representative of modern transport aircraft, as well as presenting a more challenging case for NLF design.

As with the initial supersonic case in the previous subsection of the paper, the first design case is a CDISC-only design to target pressures generated from the "best-fit" script using the SSNLF constraint. The primary purpose for this design is to evaluate the SSNLF pressure architecture and newly developed design rules in the context of turbulent flow design. The D0 airfoil was designed with an older set of CDISC constraints and a different flow solver. While it should still be a good baseline, it is hoped that the new design capability will provide an improvement even without the SOUP optimization. An additional purpose in finding the best-fit targets is to provide a starting point for the optimization that is close to the baseline, allowing the design variable changes to begin earlier in the process.

For this constraint, the best fit procedure adjusts X_{ca} and X_{shk}, as well as the UDF parameter (see figure 4). The results for the CDISC-only design to the best-fit targets (UDF = 0.18) are shown in figures 19-21. The C_L convergence band for these airfoil design cases was ±0.002 from the baseline value of 0.7, though the lift value at the minimum drag cycle was well within that tolerance. As with the MUD best-fit case, the design converged quickly, reached a flat minimum by cycle 24 as seen in figure 20, and produced a drag reduction of 7.4 counts relative to the baseline. Because the flow solver angle of attack was close to zero and held constant during the design, the raw and corrected drag values are nearly identical. For reference, the original baseline run required the equivalent of 42 design cycles to converge to the desired C_L value of 0.7. The baseline and design pressures are shown in figure 21 and indicate the drag reduction was obtained

by weakening the shock and shifting it slightly forward. The best-fit target pressures (not shown) were nearly identical to the final design pressures.

Comparing these results with those from [15], the above best-fit design did better than a prior CDISC design that used 37 manual adjustments to the target pressures (6.2 drag count reduction) and almost as good as numerical optimization (8.5 drag count reduction). It should be noted that the baseline D0 airfoil was designed using an Euler flow solver with an iterative integral boundary layer method and, when analyzed with Navier-Stokes methods in [15] as well as the current study, had a stronger shock that was further aft than in the original design, thus leading to a larger potential for drag improvement.

The next case starts from the best-fit targets, but turns on SOUP to optimize the UDF value to try to further reduce the drag. The lift convergence plot (figure 22) shows that starting from the best-fit targets allowed the optimization to start by cycle 20 and the design C_L was very closely matched by the end of the design. Figure 23 shows that the drag reached a shallow normal minimum at cycle 43, corresponding to a UDF value of 0.31. The drag reduction at this cycle, 8.7 counts, is slightly better than the best optimization case from [15]. The pressures for this case are plotted in figure 24, indicating nearly shock-free flow.

A concern with shock-free designs in the past, and single-point optimization in general, is that the off-design performance can be compromised. Part of the CDISC design philosophy in the past has been to look at what aspects of the design lead to poor off-design performance and to include this knowledge in the design approach. This would include items such as airfoil surface curvature limits, pressure gradient restrictions, and selection of the best single design point conditions. To evaluate how the SOUP optimization might affect this approach, drag polars were run at the design Mach number for a range of lift coefficients representative of the variation at cruise for the baseline, best-fit design, and SOUP optimization airfoils. The resulting drag polars are shown in figure 25, with a typical range of cruise lift coefficients (design $c_l \pm 10\%$) indicated by the black dashed lines. All three airfoils show a drag bucket at the design c_l, indicating that they are somewhat point designs. The best-fit design, however, generally has lower drag than D0 across the cruise range, with an average reduction of 3.2 counts relative to the baseline airfoil. The SOUP optimization airfoil had the lowest drag almost everywhere in the cruise range, with an average reduction of 5.4 counts relative to D0.

The final airfoil optimization case shifts from turbulent to laminar flow design. As noted in the Methods section, the design variable for NLF cases is the location of transition, X_{tr}, and the UDF value required to cause the flow to transition at this point is computed automatically within CDISC. For 3D wing designs with sweep, the X_{ca} variable is also computed by a design rule in CDISC to create the steep acceleration near the leading edge needed to attenuate the crossflow. As this is a 2D airfoil design with no sweep, crossflow attenuation is not needed, so the value of X_{ca} is kept at the typical turbulent design x/c value equal to about half of the airfoil maximum thickness-to-chord ratio. The shock location, X_{shk}, is also determined by the same rule used for turbulent flow.

A value of $X_{tr} = 0.2$ was selected to start the design. The convergence history plots in figures 26 and 27 indicate that it took more than 30 design cycles to get the design close enough to the initial targets to allow SOUP to start altering the transition location. A drag minimum was found at cycle 77, corresponding to a transition location of 0.42 and a drag reduction of 25.0 counts relative to the turbulent baseline. It appears that pushing the transition location aft of this point increases the shock Mach number and the associated wave drag, overriding the drag reduction from the longer extent of laminar flow. As with the turbulent design, the drag minimum is a fairly shallow one, with less than one count of variation over the last 28 cycles. This suggests that there may be some latitude in limiting the extent of laminar flow if it seems needed to improve the off-design performance or for nonaerodynamic reasons such as access panels.

The pressure distributions for the baseline and at design cycle 77 are shown in figure 28. The pressure gradient is nearly flat back to the transition location, where it changes to slightly adverse as it continues to the shock. The shock appears to be similar in strength to the one for the baseline, indicating that most, if not all, of the drag benefit comes from the reduced skin friction and profile drag. Examination of the pressures from later cycles showed that a more favorable gradient, with a stronger terminating shock, was required to push transition further aft.

These cases were useful in the development of the CODISC process and give an indication of both its effectiveness and efficiency for laminar and turbulent transonic design. The method gave drag reductions comparable to those obtained using standard numerical optimization, and did so in times ranging from about half to twice the time required for the baseline analysis. In addition, the best-fit approach seems to provide a good starting point for design if the baseline has reasonably good performance.

Transonic wing best-fit assessment

For a 3D wing, the CDISC knowledge base would suggest that a well-designed wing has a spanwise variation in UDF value, with higher values near the root. Therefore, the best-fit script was applied to the Common Research Model (CRM) [16] to get a quantitative assessment of this assumption. A planform view of this configuration is shown in figure 29, with the design stations shown as black lines. The best-fit script was run using the SSNLF constraint and the resulting spanwise distribution of UDF shown in figure 30. The results are similar to the NJWB best-fit case, in that the optimum values form a somewhat triangular distribution with a value near zero at the tip, though the fit is not as close as it was for the supersonic case. However, this does suggest that a scaling of this triangular distribution based on total drag could be a viable optimization strategy for transonic wings as well and an evaluation of this approach is included in the companion paper by Lynde. The resulting baseline and best-fit target pressures at an inboard and an outboard design station are shown in figures 31a and 31b, respectively. The best-fit pressures give a very close approximation to the baseline distributions, even better than with the D0 airfoil, confirming that the pressure architecture created by the SSNLF constraint should provide a reasonable starting point for optimization.

A CDISC-only design was run using the best-fit UDF values shown by the circles in figure 30, with the resulting design history results shown in figures 32 and 33. It should be noted that, even though the UDF values are held constant, the CDISC design process will still alter the target pressures based on other design rules in the SSNLF constraint, as well as changes to the current analysis pressures caused by the geometry constraints. In figure 32, the lift can be seen to enter the convergence band in less than 10 cycles because of the close match of the baseline and initial target pressures. The UDF value plotted is for station 2 and remains constant throughout the design as required. The corrected drag value approaches the baseline value (figure 33) near design cycle 10, then continues a slow growth until the process stops at cycle 34. The growth parallels an increase in the lift toward the design value of 0.5, indicating that the lift correction to the drag does not fully compensate for the lift offset. The drag of the design, however, remains within 1 count of the baseline level over the final 25 cycles, confirming that the pressure architecture and design rules developed for the SSNLF constraint using 2D cases remain viable for transonic turbulent design in a 3D environment. Optimization cases for the CRM for both laminar and turbulent flow are included in the companion paper by Lynde.

Concluding Remarks

The test cases shown in this study indicate that the CODISC design system meets the original objectives of improving the effectiveness and ease of use of CDISC without significantly increasing the time required for a CDISC-only design. Both the MUD and SSNLF constraints, for supersonic and transonic design, respectively, were shown to provide reasonable target pressure architectures with single design variables

that can effectively be adjusted using the SOUP optimizer. The "best fit" process provided a good starting point for the optimization, allowing the design variable adjustment to begin early in the process. It also led to the development of a function for the spanwise distribution of the design variable that allowed total drag reduction to drive the optimization process for 3D wing designs. The local drag optimization option did not provide any additional improvement relative to the baseline for the supersonic case, but evaluations of several modifications for this SOUP option are continuing.

The use of CODISC also led to several new design rules incorporated into the SSNLF constraint in CDISC itself. These include: 1) a rule for determining shock location that improved the stability of the design convergence; 2) an algorithm for setting the UDF parameter to match a desired transition location for laminar flow designs; and 3) a rule for adjusting pitching moment at a design station based on skin friction coefficient near the trailing edge. The best-fit function mentioned above also provided a good UDF distribution for a basic CDISC turbulent flow design for a new configuration, although a SOUP optimization would seem to be the preferred approach, as it adds little additional cost. The CODISC system appears to provide drag improvements similar to other optimization approaches in only 2-4x the time for a converged baseline analysis and, thus, represents an attractive alternative for cases where the knowledge base applies.

References

[1] Campbell, Richard L.: "Efficient Viscous Design of Realistic Aircraft Configurations," AIAA-98-2539, June 1998.
[2] Vassberg, John C.; Jameson, Antony; Peigin; Epstein, Boris; Roman, Dino L.; and Harrison, Neal A.: "A Pilot Project in Preparation of an Aerodynamic Optimization Workshop with Lessons Learned", AIAA 2008-6266, August 2008.
[3] Campbell, Richard L.: "An Approach to Constrained Aerodynamic Design with Application to Airfoils", NASA TP-3260, November 1992.
[4] Wick, Andrew T.; Hooker, John R.; Hardin, Christopher J.; and Zeune, Cale H.: "Integrated Aerodynamic Benefits of Distributed Propulsion", AIAA 2015-1500, January 2015.
[5] Wick, Andrew T.; Hooker, John R.; Walker, Jimmy; Chan, David T.; Plumley, Ryan W.; and Zeune, Cale H.: "Hybrid Wing Body Performance Validation at the National Transonic Facility", AIAA 2017-0099, January 2017.
[6] Aftosmis, M. J., Berger, M. J., and Adomavicius, G.: A Parallel Multilevel Method for Adaptively Refined Cartesian Grids with Embedded Boundaries, AIAA 2000–808, January 2000.
[7] Frink, N.T., Pirzadeh, S.Z., Parikh, P.C., Pandya, M.J., and Bhat, M.K., "The NASA Tetrahedral Unstructured Software System," The Aeronautical Journal, Vol. 104, No. 1040, October 2000, pp.491-499.
[8] Spalart, P., and Allmaras, S.A., "One-equation turbulence model for aerodynamic flows," AIAA 92-0439, January 1992.
[9] Pandya, Mohagna J.; Abdol-Hamid, Khaled S.; Campbell, Richard L.; and Frink, Neal T.: Implementation of Flow Tripping Capability in the USM3D Unstructured Flow Solver. AIAA-2006-0919, January 2006.
[10] Lynde, Michelle N. and Campbell, Richard L., "Expanding the Natural Laminar Flow Boundary for Supersonic Transports", 34th AIAA Applied Aerodynamic Conference, AIAA AVIATION Forum, AIAA 2016-4327, June 2016.
[11] Campbell, Richard L., and Lynde, Michelle N., "Natural Laminar Flow Design for Wings with Moderate Sweep", 34th AIAA Applied Aerodynamic Conference, AIAA AVIATION Forum, AIAA 2016-4326, June 2016.
[12] Lynde, Michelle N., and Campbell, Richard L., "Computational Design and Analysis of a Transonic Natural Laminar Flow Wing for a Wind Tunnel Model", 35th AIAA Applied Aerodynamic Conference, AIAA AVIATION Forum, AIAA 2017-3058, June 2017.
[13] Campbell, Richard L., and Lynde, Michelle N., "Building a Practical Natural Laminar Flow Design Capability", 35th AIAA Applied Aerodynamic Conference, AIAA AVIATION Forum, AIAA 2017-3059, June 2017.
[14] Chang, C.-L., "The Langley Stability and Transition Analysis Code (LASTRAC): LST, Linear and Nonlinear PSE for 2-D, Axisymmetric, and Infinite Swept Wing Boundary Layers," AIAA 2003-0974, 2003.
[15] Li, W.; Krist, S.; and Campbell, R.: "Transonic Airfoil Shape Optimization in Preliminary Design Environment", AIAA 2004-4629, August 2004.
[16] Vassberg, J.C. and Rivers, S.M., "Development of a Common Research Model for Applied CFD Validation", AIAA 2008-6919, August 2008.

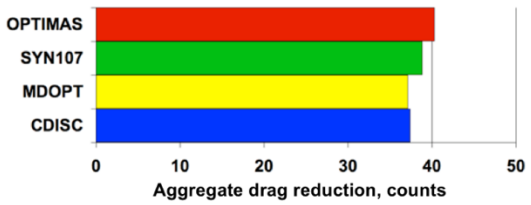

Figure 1. – Design results for mulitpoint AWODG W1 case.

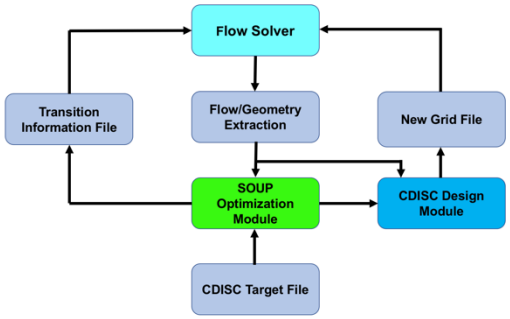

Figure 2. – Flow chart of CODISC design system.

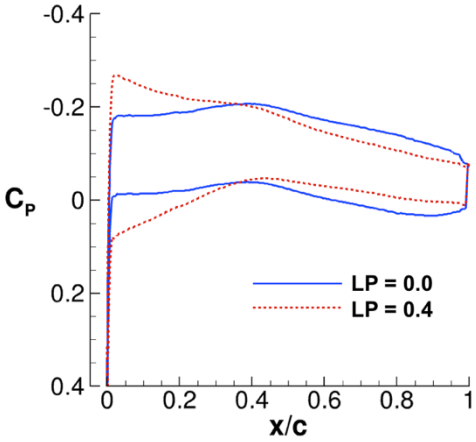

Figure 3. – Effect of MUD LP parameter on target pressures.

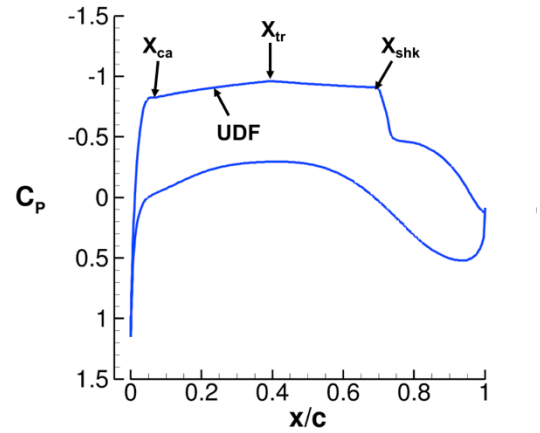

Figure 4. – SSNLF laminar target pressure architecture.

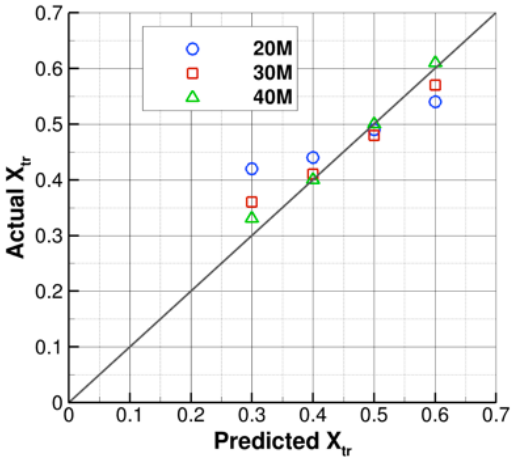

Figure 5. – Assessment of SSNLF algorithm for predicting transition location for chord Reynold numbers of 20, 30, and 40 million.

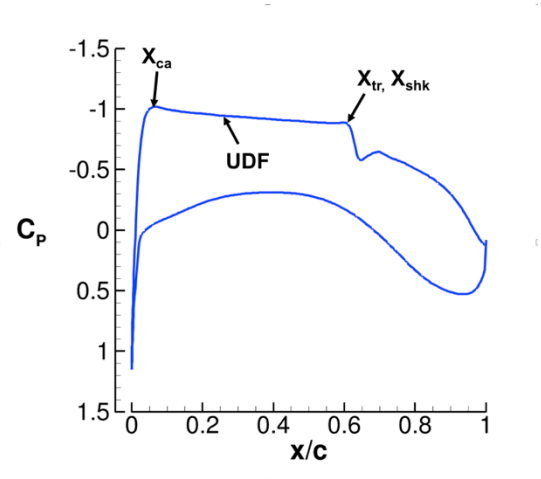

Figure 6. - SSNLF turbulent target pressure architecture.

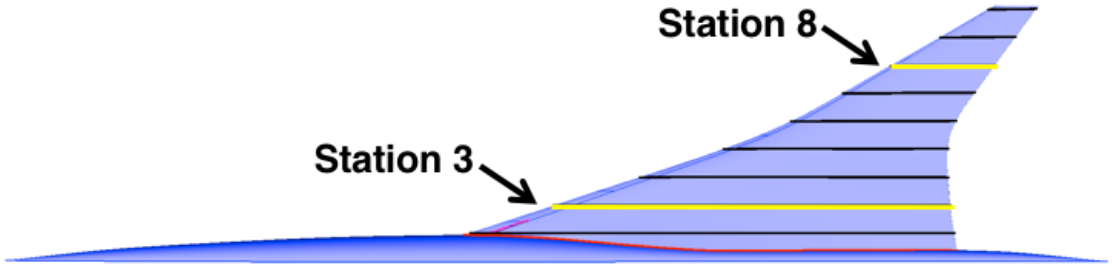

Figure 7. – NJWB planform with design stations.

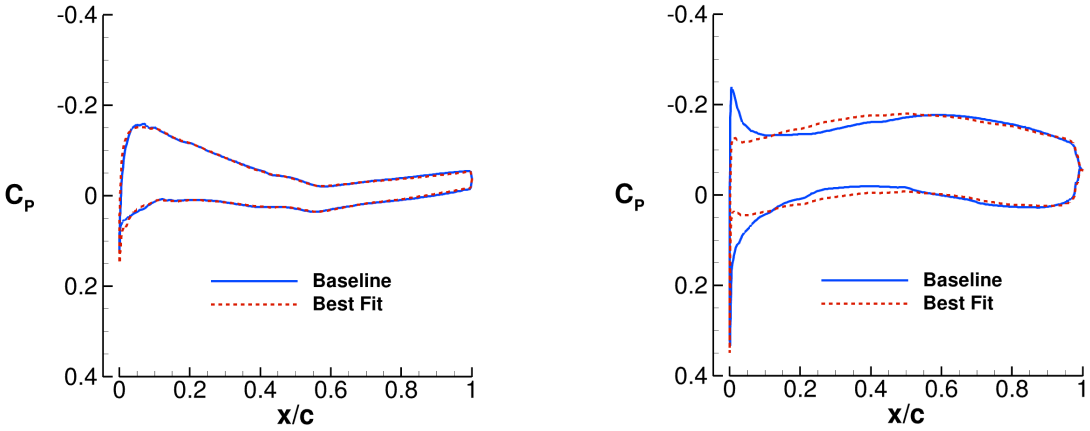

a) Design station 3.

b) Design station 8.

Figure 8. – Best fit of target pressures from MUD constraint for NJWB.

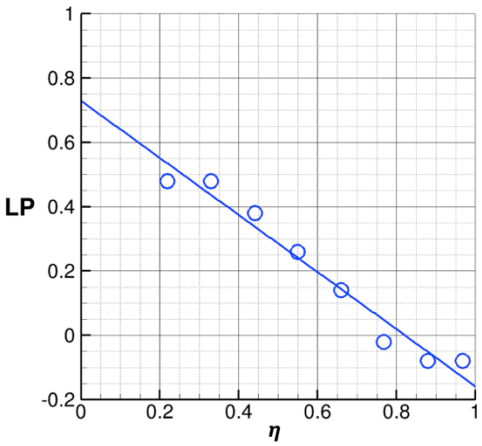

Figure 9. – Spanwise distribution of MUD loading parameter (LP) for best fit to NJWB baseline pressures.

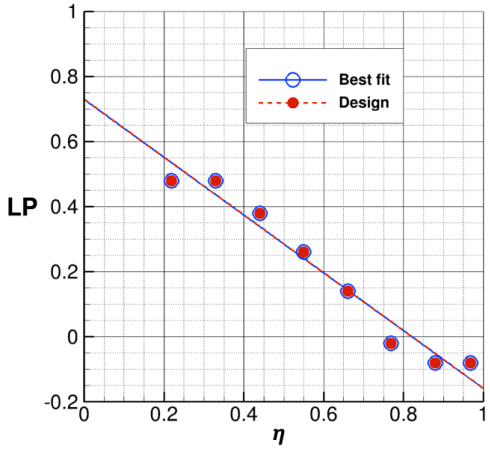

Figure 10. – LP distribution for CDISC-only design of NJWB to best-fit targets.

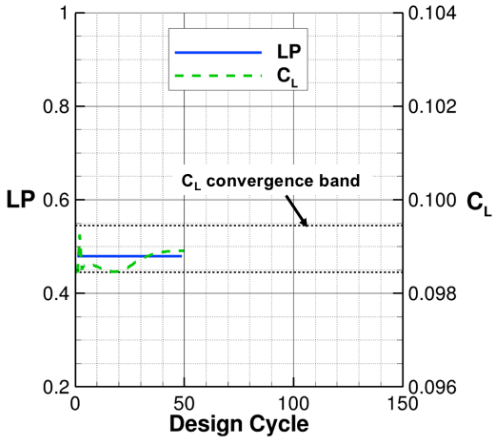

Figure 11. – Lift convergence history for CDISC-only design of NJWB to best-fit targets.

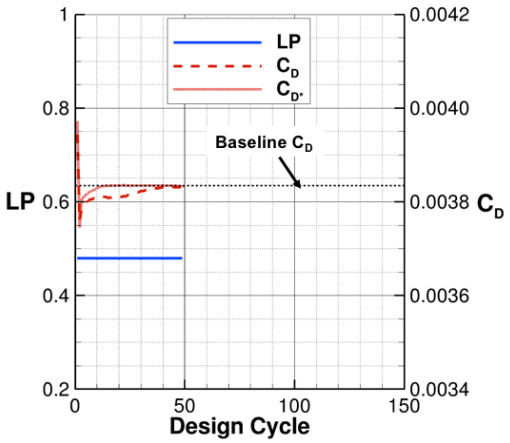

Figure 12. – Drag convergence history for CDISC-only design of NJWB to best-fit targets.

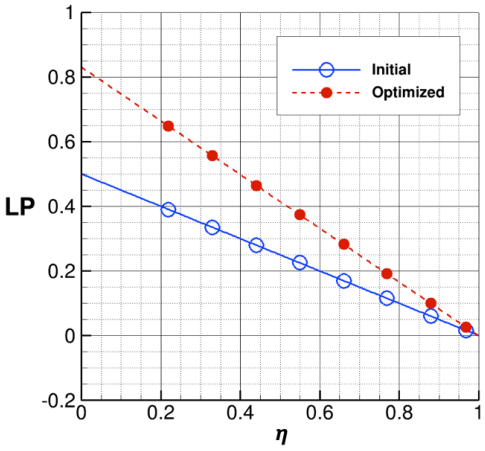

Figure 13. – LP distribution for CODISC optimization of NJWB baseline.

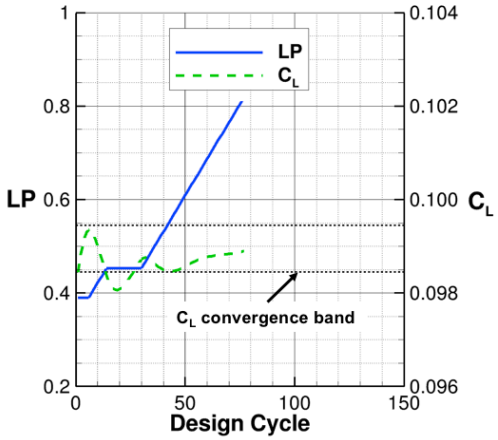

Figure 14. – Lift convergence history for CODISC optimization of NJWB baseline.

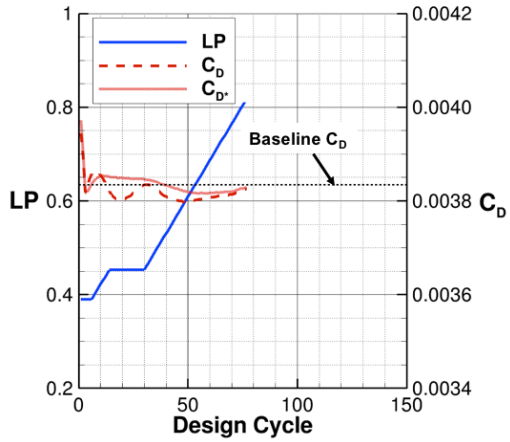

Figure 15. – Drag convergence history for CODISC optimization of NJWB baseline.

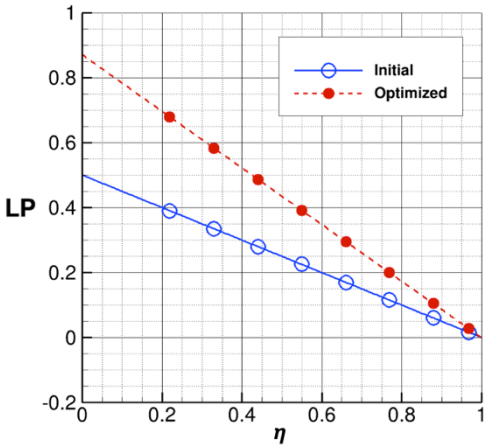

Figure 16. – LP distribution for CODISC optimization of NCT baseline.

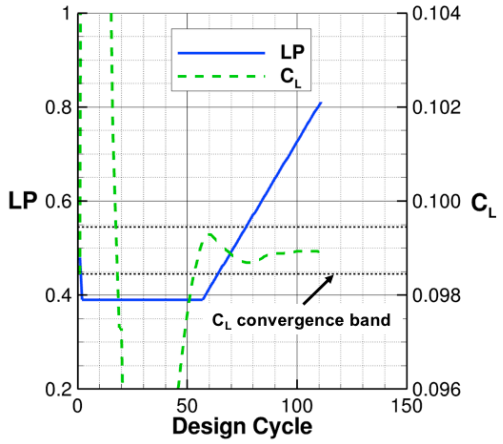

Figure 17. – Lift convergence history for CODISC optimization of NCT baseline.

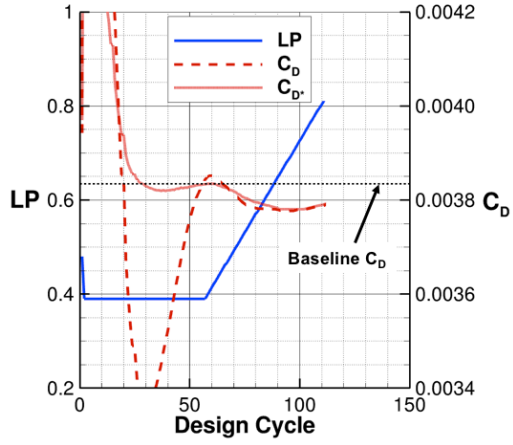

Figure 18. – Drag convergence history for CODISC optimization of NCT baseline.

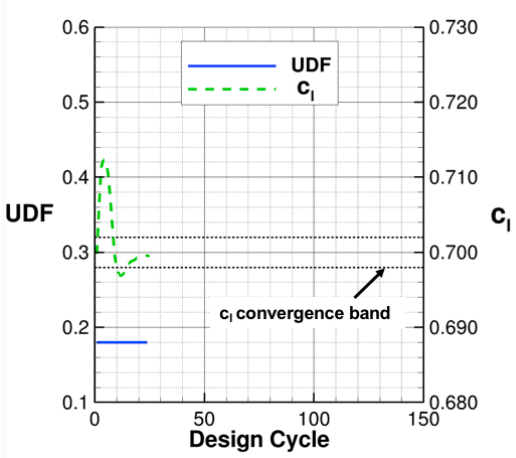

Figure 19. – Lift convergence history for CDISC turbulent design to the best-fit targets for the D0 airfoil.

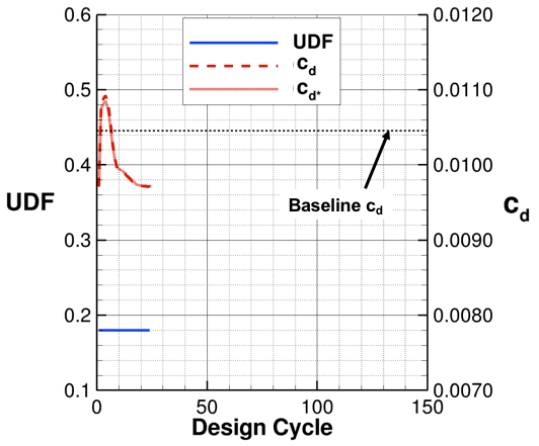

Figure 20. – Drag convergence history for CDISC turbulent design to the best-fit targets for the D0 airfoil.

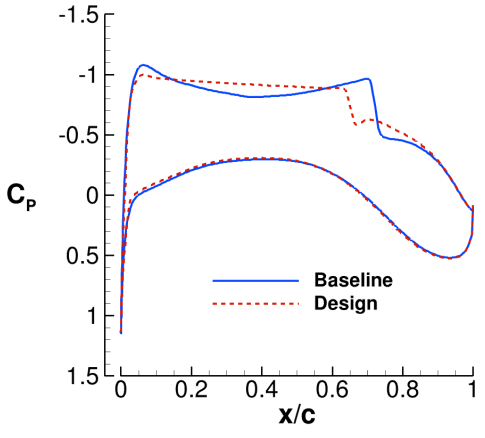

Figure 21. – Pressure results for CDISC turbulent design design to the best-fit targets for the D0 airfoil.

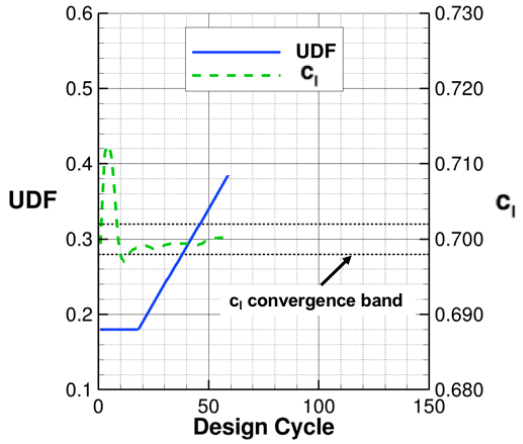

Figure 22. – Lift convergence history for CODISC turbulent optimization of the D0 airfoil.

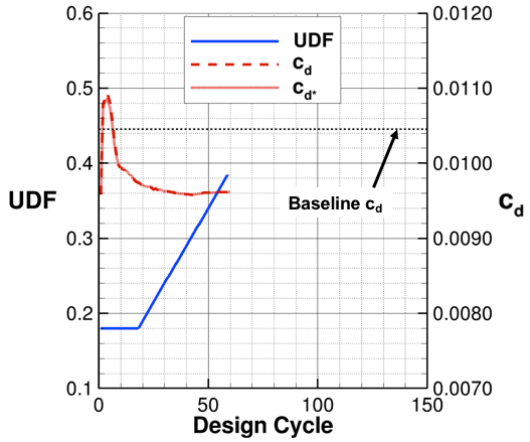

Figure 23. –Drag convergence history for CODISC turbulent optimization of the D0 airfoil.

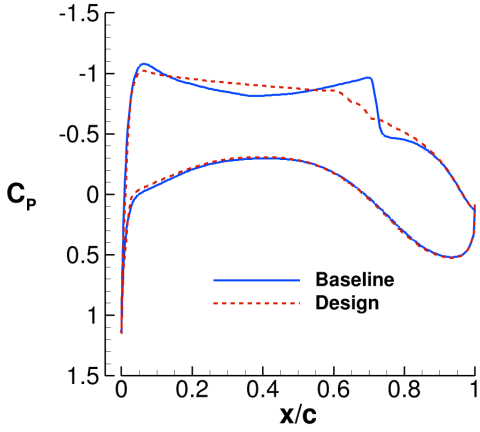

Figure 24. – Pressure results for CODISC turbulent optimization of the D0 airfoil.

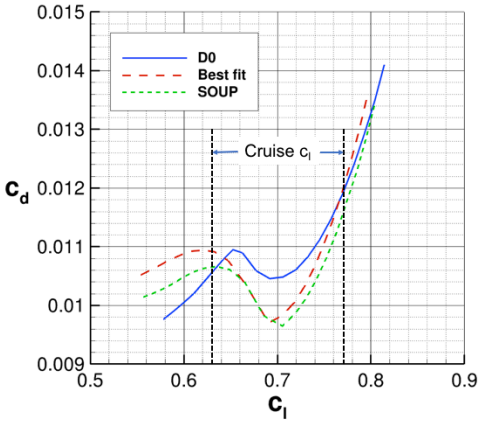

Figure 25. – Drag polars for turbulent airfoil cases.

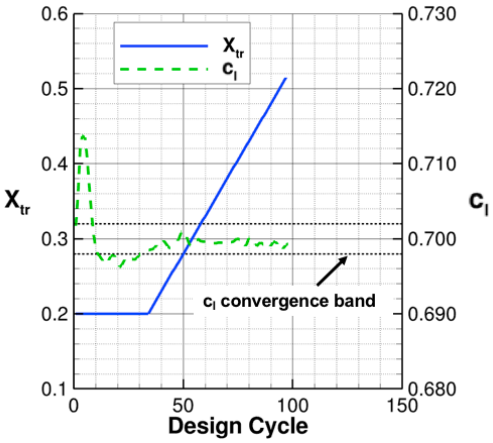

Figure 26. – Lift convergence history for CODISC NLF optimization of the D0 airfoil.

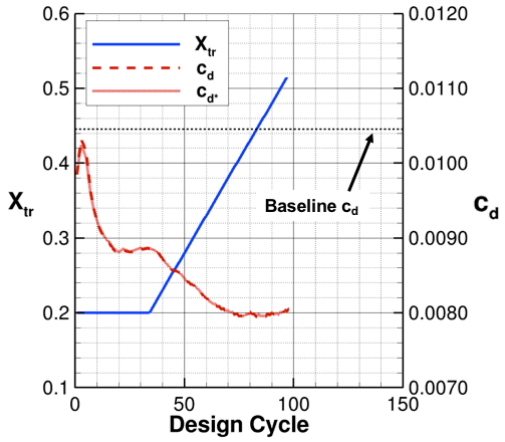

Figure 27. – Drag convergence history for CODISC NLF optimization of the D0 airfoil.

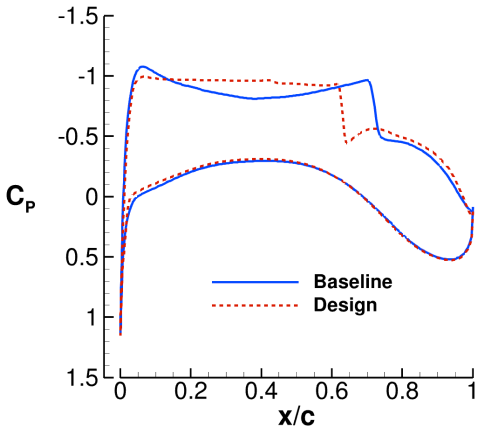

Figure 28. – Pressure results for CODISC NLF optimization of the D0 airfoil.

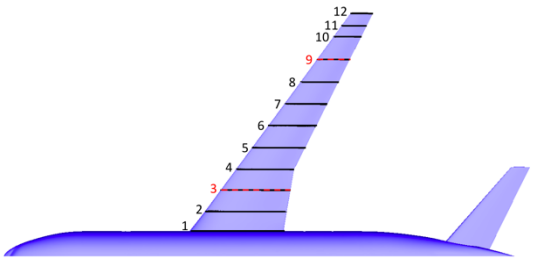

Figure 29. –CRM planform with design stations.

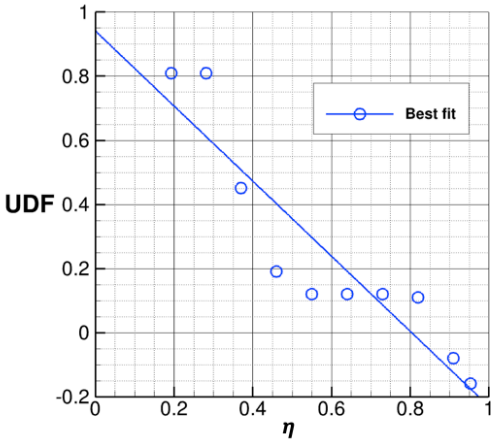

Figure 30. – Spanwise distribution of UDF for best fit to baseline CRM pressures.

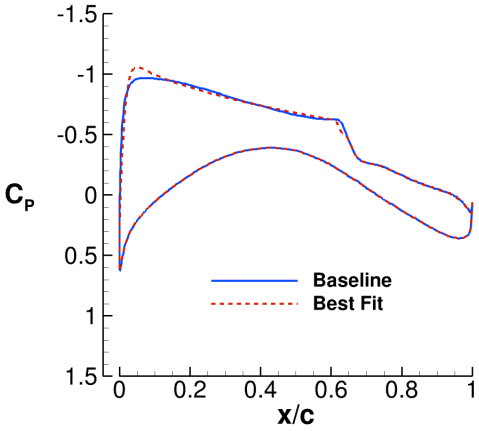

a) Station 3

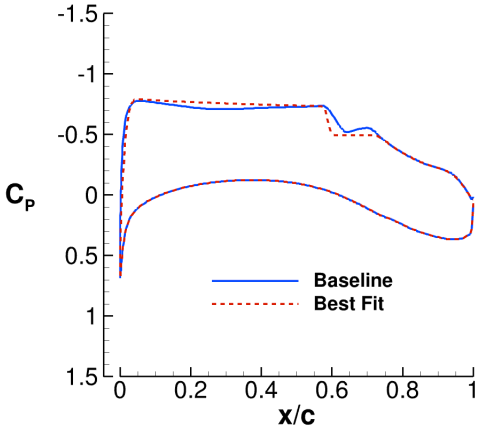

b) Station 9

Figure 31. – Best-fit target pressures for the CRM configuration.

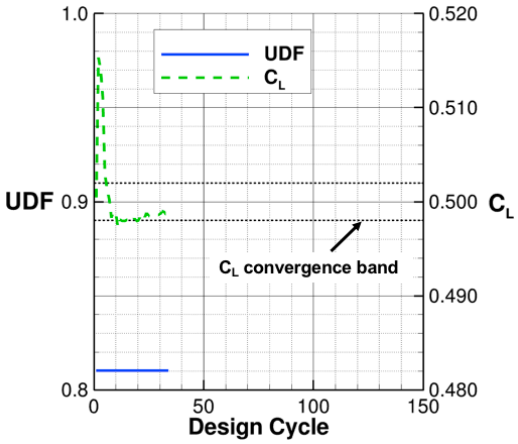

Figure 32. – Lift convergence history for CDISC-only design to CRM best-fit target pressures.

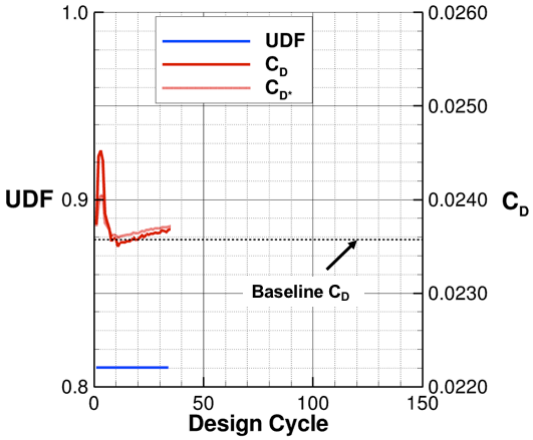

Figure 33. – Drag convergence history for CDISC-only design to CRM best-fit target pressures.